Received: 22 November 2016 | Revised: 26 June 2017 | Accepted: 27 June 2017
DOI: 10.1002/stc.2069

RESEARCH ARTICLE

WILEY

Hybrid simulation of structural systems with online updating of concrete constitutive law parameters by unscented Kalman filter

Zhu Mei[1,2,3] | Bin Wu[1,2] | Oreste S. Bursi[3] | Ge Yang[1,2] | Zhaoran Wang[4]

[1] Key Lab of Structures Dynamic Behavior and Control (Harbin Institute of Technology), Ministry of Education, Harbin 150090, China
[2] School of Civil Engineering, Harbin Institute of Technology, Harbin 150090, China
[3] Department of Civil, Environmental and Mechanical Engineering, University of Trento, Trento 38123, Italy
[4] China State Construction Technical Center, Beijing 101300, China

Correspondence
Bin Wu, School of Civil Engineering, Harbin Institute of Technology, Harbin 150090, China.
Email: wbhit@sina.com

Funding information
National Key Research and Development Program of China, Grant/Award Number: 2016YFC0701106; National Natural Science Foundation of China, Grant/Award Number: 51161120360; 7th Framework Programme of the European Commission, Grant/Award Number: [FP7/2007–2013] 227887 and FP7/2007–2013

Summary
Online model updating in hybrid simulation (HS) can represent an effective technique to reduce modeling errors of parts numerically simulated, that is, numerical substructures, especially when only a few critical components of a large system can be tested, that is, physical substructures. As a result, in an enhanced HS with online model updating, parameters of constitutive relationship can be identified based on experimental data provided by physical substructures and updated in numerical substructures. This paper proposes a novel method to identify constitutive parameters of concrete laws with unscented Kalman filter (UKF). In order to implement UKF, parts of the source codes of the OpenSEES software were modified to compute estimated measurements. Prior to experimental HS, a parametric study of UKF constitutive law parameters was conducted. As a result, the effectiveness of the UKF combined with OpenSEES was validated through numerical simulations, a monotonic loading test on a concrete column and real-time HSs of a reinforced concrete frame run with both standard and model-updating techniques based on UKF.

KEYWORDS
concrete constitutive law, hybrid simulation, online model updating, OpenSEES, unscented Kalman filter

1 | INTRODUCTION

Hybrid simulation (HS) represents an effective method to investigating the dynamic behavior of structures with large or even full-scale test prototypes in an inexpensive way.[1–4] In particular, HS isolates the physical substructures (PSs), which is experimentally tested because it contains a key region (or component) exhibiting nonlinear behavior, from the remainder of the system, which is numerically simulated, that is, the numerical substructures (NSs). As a result, no explicit dynamic model of the PS is required, and the evaluation of any internal nonlinear dynamic behavior can be experimentally examined by including the PS in the real-time—or close to real-time—substructuring loop. The test complexity depends on the problem to hand. In fact, the need to conduct efficient experimental tests of a midlevel-isolated building can require the construction and interface of a shaking table with a real-time hybrid control system.[5] Both in simple and complex HS arrangements, the accuracy of HS on representing seismic performance of components/system is mainly influenced by time delay arising from actuator control,[6–8] time integration marching schemes,[9–11] and modeling of NSs.[12,13] In this respect, several studies have been conducted for reducing error results originating from the first two issues. They are out of the scope of this research.

The modeling of NSs is based on the idealization of actual substructures, and it usually relies on the assumption that each NS is characterized by high accuracy; this is achieved especially when it remains in the linear regime. Nonetheless, some parts of NSs either because it would be uneconomical to test all critical components in a laboratory or due to significant earthquake excitation levels will, in general, exhibit a nonlinear behavior. As a result, nowadays, a lot of effort is devoted to modeling NSs and, in particular, on online model updating. In a greater detail, the behavior of NSs is modified during the test based on data obtained from PSs, provided that both the source and the modified substructures share close characteristics.[14,15] For instance, in order to improve the accuracy of NS modeling, Nakano and Yang[16] adopted neural networks rather than a finite element (FE) model. Thus, a NS was trained online, that is, updated with experimental data. The "black-box" of the relevant neural network resulted in a significant number of hidden layer nodes, that is, the main factor that influenced accuracy. Moreover, also the computation burden increased along with the number of hidden layer nodes, making the neural network unfeasible for HS. Along this line, also constitutive laws were extensively investigated and used in FE software; it is clear that the determination of constitutive relationship parameters plays an important role on simulation accuracy, indeed.[17,18] Consequently, late research in HS is giving great emphasis on the identification of constitutive laws characterized by a limited number of parameters.

In structural analysis, typically three levels of constitutive relationships are involved: (a) the component level characterized by a force-displacement law; (b) the section level typically described with a moment-curvature relation; (c) the material level associated to a stress–strain relationship. In the framework of HS, the most widely relationship adopted for model updating is the one at the component level. For instance, Yang et al.[14] accomplished a HS on a bridge with two steel-concrete composite piers by means of model updating, where the Bouc–Wen model was adopted for simulating the hysteretic behavior of one pier, that is, the PS and its parameters were identified. Wu and Wang[19] conducted a HS on a braced frame in which the nonlinear behavior of a buckling-restrained brace was also described by a Bouc–Wen model with updated parameters. Also, Shao and coworkers[20] carried out a HS on a three-story shear-type steel building. The first floor was physically tested and the upper two stories were numerical simulated by a Bouc–Wen model, whose parameters were identified and updated.

When one deals with reinforced concrete (RC) members, for example, piers, columns, beams, and so forth, existing Bouc–Wen models used at the component level appear to be not appropriate. In fact, the limited number of parameters present in a Bouc–Wen model is not enough to represent the marked nonlinear behavior of members of different size, reinforcement ratio, axial compression ratio, etc. As a result, Wu et al.[21] proposed to update a section constitutive model and verified it by a HS on a steel frame. Nonetheless, this approach appears to be inaccurate for inelastic RC members; thus, online model updating was directly applied to stress–stain relationships that characterize fiber-based elements.

In the field of state and parameter estimation, Kalman filter[22] is the most widespread method for linear systems. As an extension to nonlinear systems, the unscented Kalman filter (UKF)[23–25] has attracted significant attention for parameter identification, because is more computationally efficient and robust than many nonlinear optimization methods. In this respect, Hashemi et al.[15] illustrated the implementation of online model updating in HS with UKF for a Bouc–Wen model; it was used as constitutive law of rotation spring in a concentrated plastic model of a frame column. Likewise, the estimation methods adopted in Yang et al.,[14] Wu and Wang,[19] and Wu et al.[21] were all based on UKF.

Notwithstanding the literature available on model updating and its implementation in HS, procedures and software that allow for developing credible nonlinear FE codes of RC structural systems based on model updating of critical NSs are still at their embryonic stage. Therefore, in this paper, we propose to carry out HS based on the updating of NSs at the constitutive level, with relevant parameters identified by UKF. In order to implement UKF for simulation of nonlinear concrete members, the OpenSEES software[26] was properly modified to compute estimated measurements. As a result, hereinafter, we show the effectiveness of model updating based on both UKF and OpenSEES through pure numerical simulations, a monotonic loading test on an RC concrete column, and a HS on a one-bay one-story RC frame, respectively. The HS was carried out with both standard and model-updating techniques based on unscented Kalman filter.

2 | CONSTITUTIVE PARAMETERS OF CONCRETE FOR IDENTIFICATION

In RC structures, the uncertainty in concrete material values is obviously greater than that in reinforcing steel bars (rebars); therefore, this paper focuses on identifying and updating the parameters of concrete constitutive law. In particular, we will focus on the updating of uniaxial constitutive relationships that characterize fibers of FE-based fiber elements.

2.1 | Uniaxial constitutive model

Figure 1 shows the stress–strain relationship of the concrete model defined in OpenSEES,[26] that is, the Kent-Scott-Park model.[27,28] It can be expressed as

$$\begin{cases} \sigma = f_c\left[\frac{2\varepsilon}{\varepsilon_0} - \left(\frac{\varepsilon}{\varepsilon_0}\right)^2\right], & \text{ascending branch} \\ \sigma = f_c + \frac{f_r - f_c}{\varepsilon_m - \varepsilon_0}(\varepsilon - \varepsilon_0), & \text{descending} \end{cases}, \tag{1}$$

in which f_c is the axial compressive strength; ε_0 is the strain at the compressive strength; ε_m defines the crushing strain; f_r is the strength corresponding to strains equal or greater than ε_m. The compressive strength and strain confined by stirrups are related to the corresponding unconfined parameters[27,28] through

$$f_c = (1 + K_{sr1}\rho_s)f_{cu}, \tag{2}$$

$$\varepsilon_0 = (1 + K_{sr1}\rho_s)\varepsilon_{0u}, \tag{3}$$

where ρ_s is the volumetric ratio of stirrup; f_{cu} and ε_{0u} define the compressive strength and strain for unconfined concrete, that is, $\rho_s = 0$; and

$$K_{sr1} = f_{yh}/f_{cu}, \tag{4}$$

in which f_{yh} is the yield strength of stirrups. As an alternative to the the Kent–Scott–Park model, Mander et al.[29] suggested that stirrups entail stronger confining effects on strains than on strengths, and thus, different formula were suggested for ε_0, that is,

$$\varepsilon_0 = (1 + K_{sr2}\rho_s)\varepsilon_{0u}, \tag{5}$$

where

$$K_{sr2} = 5K_{sr1}. \tag{6}$$

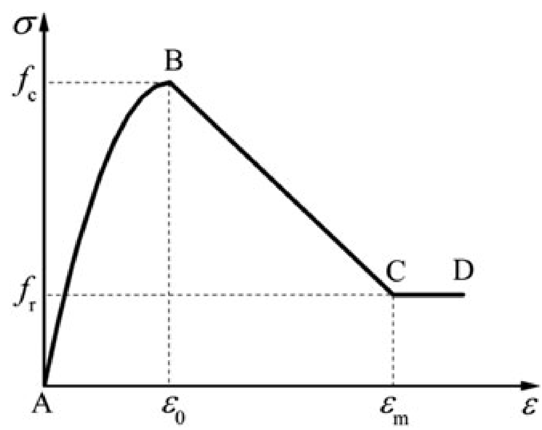

FIGURE 1 Kent–Scott–Park concrete model available in OpenSEES[26]

Similarly, the crushing strain can be expressed as[27]

$$\varepsilon_{\rm m} = (1 + K_{\rm sr3} \cdot \rho_{\rm s})\varepsilon_{\rm mu} \tag{7}$$

in which

$$K_{\rm sr3} = \frac{0.9 f_{\rm yh}}{300 \times 0.004}. \tag{8}$$

Kent[28] proposed a different model for determining crushing strain. The crushing strength f_r was assumed as a fraction of compressive strength, that is,

$$f_{\rm r} = K f_{\rm c}. \tag{9}$$

In this respect, Hognestad[30] suggested 85% for K, whereas other researchers proposed figures between 50% and 80% based on experimental data.

From the analysis presented above, the basic constitutive parameters that characterize a stress–strain relationship are f_{cu}, ε_{0u}, ε_{mu}, and f_{ru}. Some of those can be determined from material tests on unconfined concrete, and others can be calculated from 2, 5, 7, and 9, respectively. However, there are still uncertainties associated with the determination of these parameters and as well as those for confined concrete. Therefore, in view of parameter identification, K_{sr1}, K_{sr2}, and K_{sr3} can be considered as independent constitutive parameters, whereas K can be determined from 9 together with f_{cu} and f_{ru}. In sum, stress can be expressed as a function of strain by means of seven constitutive parameters and the volumetric ratio of stirrups ρ_s, that is,

$$\sigma = g(\varepsilon, f_{\rm cu}, \varepsilon_{\rm 0u}, f_{\rm ru}, \varepsilon_{\rm mu}, K_{\rm sr1}, K_{\rm sr2}, K_{\rm sr3}, \rho_{\rm s}) \tag{10}$$

2.2 | Sensitivity analysis of constitutive law parameters

In order to analyze the influence of concrete constitutive parameters on restoring force of a RC component, a sensitivity analysis of parameters was carried out. In this respect, a RC free-fixed column was modeled in OpenSEES using a force-based element with five integration points evenly distributed along its height of 1,200 mm. The RC column was equal to the prototype used for experimental validation in subsection 3.2.2. The cross section of the column is shown in Figure 2. A fiber section was used for the cross-sectional model, and the discretization is presented in Figure 3, where circles denote the fibers of steel rebars. Their nonlinear behavior was reproduced by the Giuffre–Menegotto–Pinto model, that is, material Steel02 of OpenSEES.[26] Confined and unconfined concrete are defined by material Concrete01, that is, the Kent–Scott–Park model.[27,28]

The volumetric ratio of stirrups ρ_s was assumed to be 0.34% with the reference values of concrete constitutive parameters,

$$\mathbf{P} = [f_{\rm cu} \;\; \varepsilon_{\rm 0u} \;\; f_{\rm ru} \;\; \varepsilon_{\rm mu} \;\; K_{\rm sr1} \;\; K_{\rm sr1} \;\; K_{\rm sr1}] = [24 \quad 0.002 \quad 17 \quad 0.004 \quad 18 \quad 18 \quad 141].$$

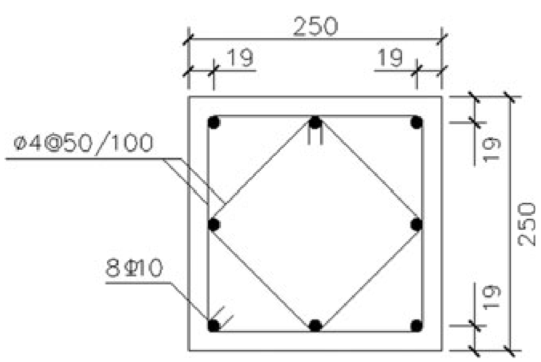

FIGURE 2 Cross section of a prototype column

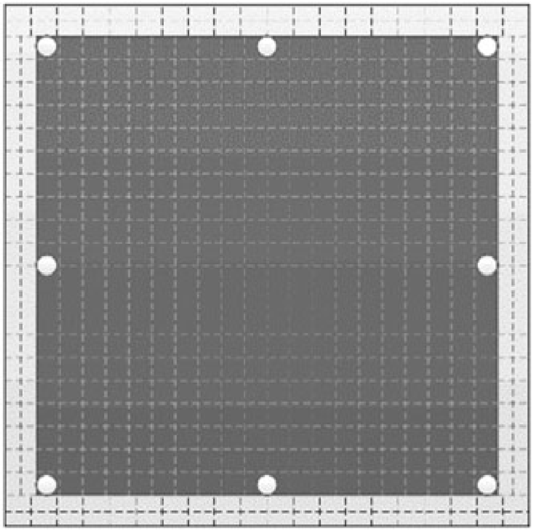

FIGURE 3 Section of finite element model by OpenSEES. Dark and light gray parts represent confined and unconfined concrete

The column was then subjected to a lateral load of 200 kN in displacement control. Several runs were made to introduce a variation of constitutive parameters up to 40%. As a result, Figure 4 shows both the column restoring force and relative variation of most sensitive parameters among the seven under investigation. An attentive reader can clearly observe that the restoring force is mainly sensitive to f_{cu}, ε_{0u}, and f_{ru}. Hence, the remainder of the paper will focus on the identification of these parameters.

3 | PARAMETER IDENTIFICATION BY UKF AND VALIDATION

3.1 | UKF for nonlinear estimation and implementation

Let **x** denote the parameter vector of constitutive relationship for concrete, that is,

$$\mathbf{x} = [f_{cu}, \varepsilon_{0u}, f_{ru}], \tag{11}$$

which is related to the measurement vector **y** through

$$\mathbf{y} = \mathbf{h}(\mathbf{x}) + \mathbf{v}, \tag{12}$$

where **y** is an m-dimensional measurement vector, and **v** a noise vector with the same dimension. For stochastic estimation of **x**, which can be generally view as a random vector, Doob[31] proved that the optimal estimation with the mean-square-error criterion corresponds to the conditioned mean given **y**, that is, $\widehat{\mathbf{x}}_{opt} = \mathrm{E}(\mathbf{x}|\mathbf{y})$.

For linear systems, where **h** is a linear function of **x**, Kalman[22] proposed a method whose estimation exactly corresponds to the above-mentioned optimal estimation. It was named Kalman filter, where the gain estimation required only the first two orders of statistic moments about **x** and **y**. Nonetheless, for nonlinear systems, the knowledge of the first two orders of statistic moments is not sufficient to determine optimal estimation. Although the conditional mean could be determined with the conditional probability distribution function, the computation effort involved could be significant. In order to avoid these burdens, one can retain the linear structure of Kalman filter and approximate the first two moments. Therefore, the estimation of **x** can be expresses as

$$\hat{\mathbf{x}}_i = \hat{\mathbf{x}}_{i-1} + \mathbf{K}_i(\mathbf{y}_i - \hat{\mathbf{y}}_i), \tag{13}$$

where $\mathbf{K}_i$ defines the gain at step i. The approximation of mean and covariance in UKF can be carried out with a deterministic sampling method. As a result, the sampling points with the scaled symmetric unscented transformation can be expressed as[23,24]

$$\chi_j^i = \begin{cases} \hat{\mathbf{x}}_{i-1}, & j = 0 \\ \hat{\mathbf{x}}_{i-1} \pm \alpha \left(\sqrt{n \mathbf{P}_{\hat{\mathbf{x}}\hat{\mathbf{x}}}^i} \right)_j, & j = 1, 2, \ldots n \end{cases}, \tag{14}$$

where n is the dimension of $\mathbf{x}$, χ_j^i is called sigma points whose total number is $2n + 1$ at the ith step. Following the nonlinear transformation the corresponding points ξ_j^i can be obtained by means of $\xi_j^i = \mathbf{h}_i\left(\chi_j^i\right)$, and then, the approximated $\mathbf{y}$ and $\mathbf{P}_{\hat{\mathbf{y}}\hat{\mathbf{y}}}$ can be calculated as

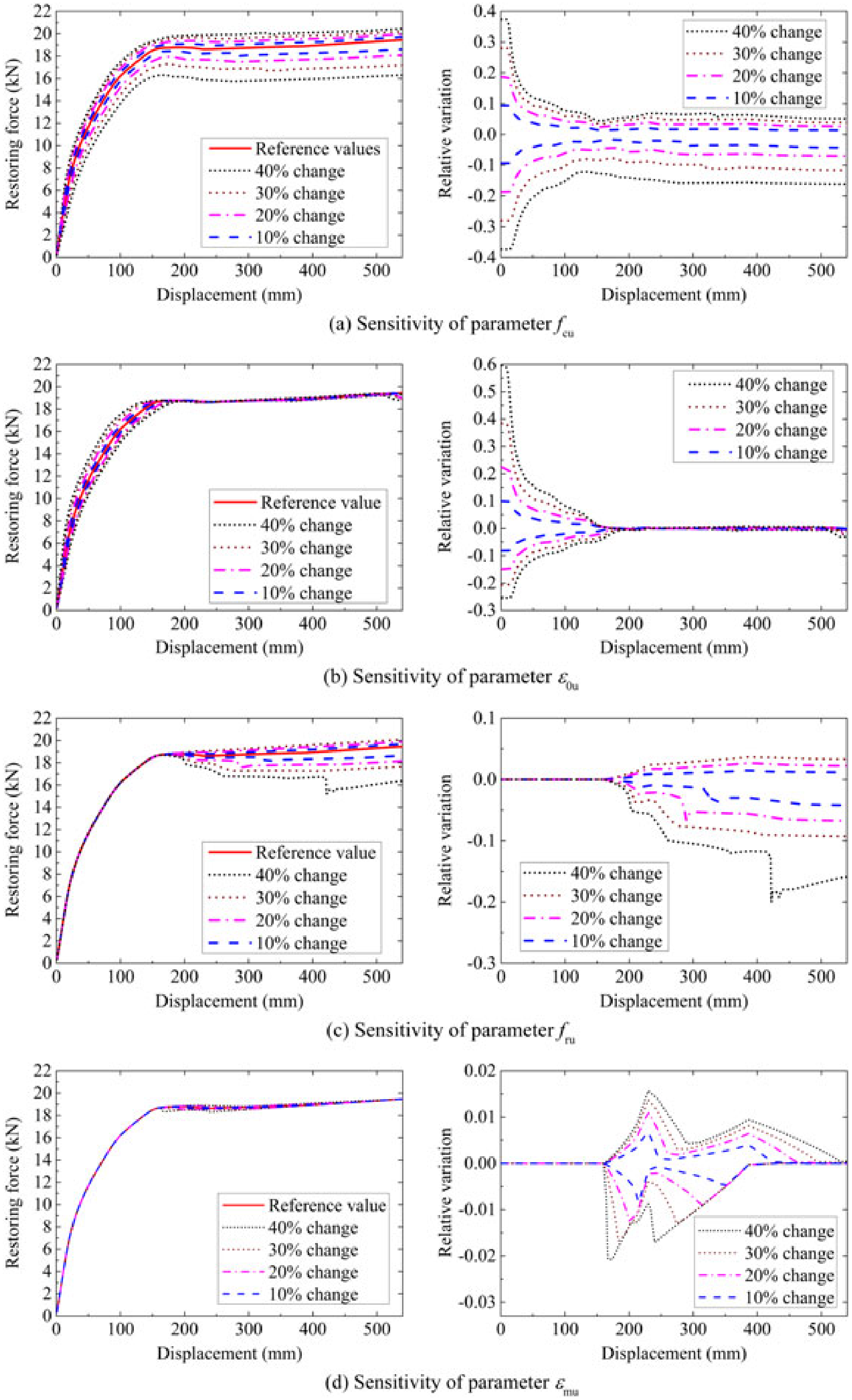

(a) Sensitivity of parameter f_{cu}

(b) Sensitivity of parameter ε_{0u}

(c) Sensitivity of parameter f_{ru}

(d) Sensitivity of parameter ε_{mu}

FIGURE 4 Sensitivity of restoring force of a free-fixed end column to concrete constitutive law parameters

$$\hat{\mathbf{y}}_i = \sum_{j=0}^{2n} W_j^{\mathrm{m}} \boldsymbol{\xi}_j^i, \tag{15}$$

$$\mathbf{P}_{\hat{\mathbf{y}}\hat{\mathbf{y}},\mathrm{i}} = \sum_{j=0}^{2n} W_j^{\mathrm{c}} \left[\boldsymbol{\xi}_j^i - \hat{\mathbf{y}}_i\right]\left[\boldsymbol{\xi}_j^i - \hat{\mathbf{y}}_i\right]^{\mathrm{T}}, \tag{16}$$

where, W_j^{m} and W_j^{c} define the weight coefficients for mean and variance, respectively, that is, $W_0^{\mathrm{m}} = 1 - 1/\alpha^2$, $W_0^{\mathrm{c}} = W_0^{\mathrm{m}} + 1 - \alpha^2 + \beta$, and $W_j^{\mathrm{m}} = W_j^{\mathrm{c}} = 1/(2n\alpha^2)$, $j \neq 0$. For a Gaussian distribution of a scalar x, an accuracy of fourth order for the mean and covariance of $\mathbf{y}$ can be achieved with $\alpha^2 = 3$ and $\beta = \alpha^2 - 2/3 = 7/3$, respectively.

For the identification of concrete constitutive parameters in a HS, measurement is typically represented by the restoring force of a concrete member. Hence, the corresponding points $\boldsymbol{\xi}_j^i$ of estimated measurement in 15 could not be directly computed given the complex relationship $\mathbf{h}$ in 12, between measurement and constitutive parameters. As a result, the OpenSEES software was employed to calculate the corresponding points after nonlinear transformations based on sigma points $\boldsymbol{\chi}_j^i$, historical variables and inputs, that is,

$$\boldsymbol{\xi}_j^i = \mathbf{h}\left(\boldsymbol{\chi}_j^i, \mathbf{r}_{i-1}, \mathbf{u}_i\right), \tag{17}$$

where $\mathbf{u}_i$ defines the vector of displacements as input and $\mathbf{r}_{i-1}$ is the vector of historical variables generated by OpenSEES computed at Step i-1. Note that the computation with different samples of parameters results in different sets of new historical variables, which can be used as part of the input for the next step. However, it is apparent that only one set of historical variables should be used. To address this problem, an extra running of OpenSEES with the new estimated parameters at step i, that is, $\widehat{\mathbf{x}}_i$, was executed to obtain the unique set of historical variables for the next step.

The UKF identification algorithm was implemented through MATLAB[32] wheras OpenSEES was employed to calculate the corresponding points of the predicted measurement based on $\boldsymbol{\chi}_j^i$ generated by the main program. The flow chart of the whole identification process is depicted in Figure 5.

The communication between MATLAB and OpenSEES is realized by a TCP/IP protocol for which the relevant code is written in C++ language and embedded in MATLAB. Some source codes in OpenSEES were modified to run the software with sampled or updated concrete parameters. Note that for each set of constitutive parameters, extra source codes should be included to enable OpenSEES to run with the same historical variables determined at the end of last time step. The main parts of the modified source codes are Concrete01 in the material part; ForceBeamColumn2d in the element part, Domain part, and Tcp-socket part; and StaticAnalysis in the analysis part. Besides, a new analysis code was added to the analysis part.

3.2 | Validation of parameter identification

The validation of constitutive parameter identification was based both on data provided by the free-fixed concrete column simulated in subsection 2.2 and from a relevant monotonic test.

3.2.1 | Numerical validation

The measurement was simulated by adding samples of white noise to restoring forces obtained from the FE analysis of the column laterally loaded. The maximum value of the sampled white noise was scaled to 1% of the maximum calculated horizontal force. Table 1 provides both the initial and reference (true) values of parameters, where the initial K_{sr1} and

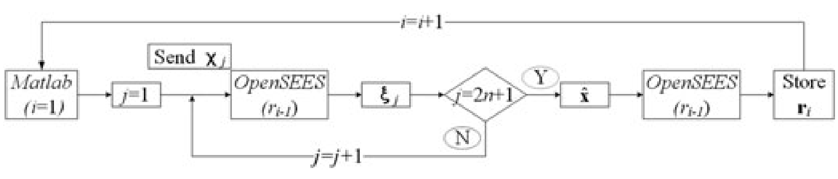

FIGURE 5 Flowchart of identification process

K_{sr3} values are given by 4 and 8 whereas the initial value of K_{sr2} is set to be 3 times K_{sr1}. For the UKF method, the covariance matrix of parameters and noise read diag$P_0 = [6\times10^{-12}\ 9.5\times10^{-13}\ 6\times10^{-11}]$ and $R = 9\times10^{-11}$, respectively.

Figure 6 shows results of identification, from which the favorable performance of the identification method is clearly seen. The force response with identified parameters almost duplicates the reference response as can be appreciated in Figure 6d. Table 2 reports the relative errors of converged values to reference ones with a maximum error level of 1.5%. The three constitutive parameters converge rapidly to reference values, although f_{ru} remains constant when the displacement is less than 20 mm. The reason for a constant f_{ru} at lower displacements is that when $\varepsilon < \varepsilon_{0u}$. f_{ru} has no effect on stresses and, hence, on force response.

It is interesting to note that f_{cu} is linearly related to the restoring force of the column; see Appendix A in this respect. If f_{cu} is the sole parameter to be estimated, then the identification problem becomes a linear one and the UKF reduces to a Kalman filter problems. In fact, it can be proved that the estimated value will monotonically converge with a Kalman filter treatment; relevant details and numerical confirmation are presented in Appendix B. However, an overshoot of f_{cu} can be observed in Figure 6a when more parameters are involved. An explanation for this trend is provided in Appendix C by means of identification of two parameters f_{cu} and ε_{0u}.

TABLE 1 Initial and reference values of concrete constitutive law parameters

Parameter	f_{cu} (MPa)	ε_{0u}	f_{ru} (MPa)	ε_{mu}	K_{sr1}	K_{sr2}	K_{sr3}
Initial value	38	0.002	32.3	0.0045	8	24	157
Reference value	28	0.0026	15.4	0.0045	8	24	157

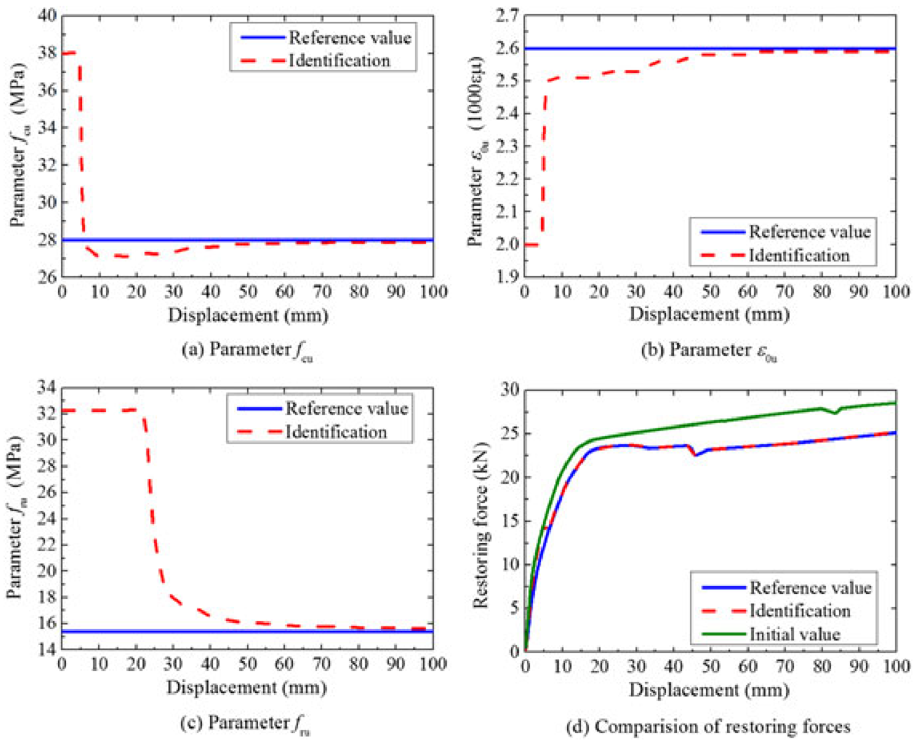

FIGURE 6 Identification results compared with simulated measurements

TABLE 2 Relative errors of both identified and initial values to reference ones

Relative errors in %	f_{cu}	ε_{0u}	f_{ru}
Initial value	35.7	23.1	110
Converged value	0.4	0.3	1.5

3.2.2 | Experimental validation

In this section, measurements for identification were obtained from a monotonic loading test of an RC column whose cross section was described in subsection 2.2. The test was performed at the Structural and Seismic Testing Center, Harbin Institute of Technology. Figures 7 and 8 present the test setup and relevant dimensions of prototype specimen, respectively.

Two Linear Variable Differential Transformer (LVDTs) were placed to measure the foundation displacement and that of column at the centerline of actuator, separately. In order to make sure that the target displacement was fully applied to the specimen, the column was controlled based on the measurement difference of the two LVDTs. The column was laterally loaded up to a displacement of 82 mm, when three significant cracks appeared with the width of about 6 mm. Relevant photos are shown in Figure 9.

In view of identification, the initial values of f_{cu} and K_{sr1} were determined from data of concrete and steel material tests, and the others were similar to those employed in section 3.2.2; these data are collected in Table 3. The initial covariance matrix for UKF is $\mathrm{diag}P_0 = [2.7 \times 10^{-2}\ 3.5 \times 10^{-6}\ 5 \times 10^{-4}]$ and R reads 9×10^{-4}, respectively.

Identification results are presented in Figure 10 from which one can deduce that a favorable performance was achieved. However, one can note that in the first few steps, the parameter f_{cu} jumped from an initial value of 43 to

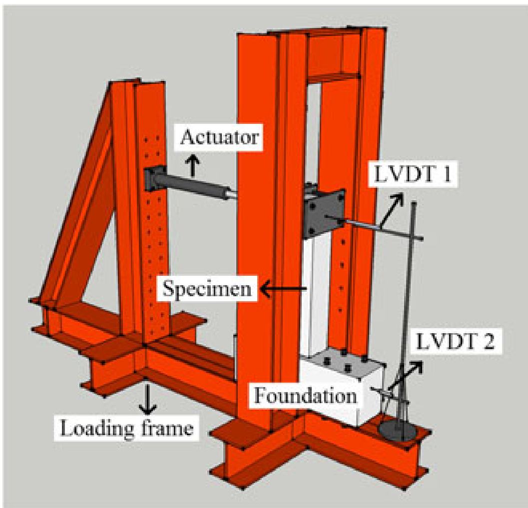

FIGURE 7 Sketch of testing equipment. LVDT = Linear Variable Differential Transformer

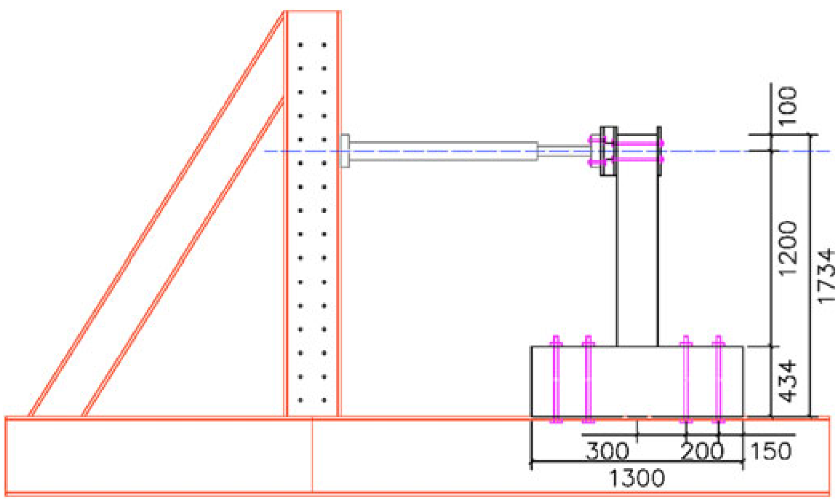

FIGURE 8 Main dimension of prototype specimen

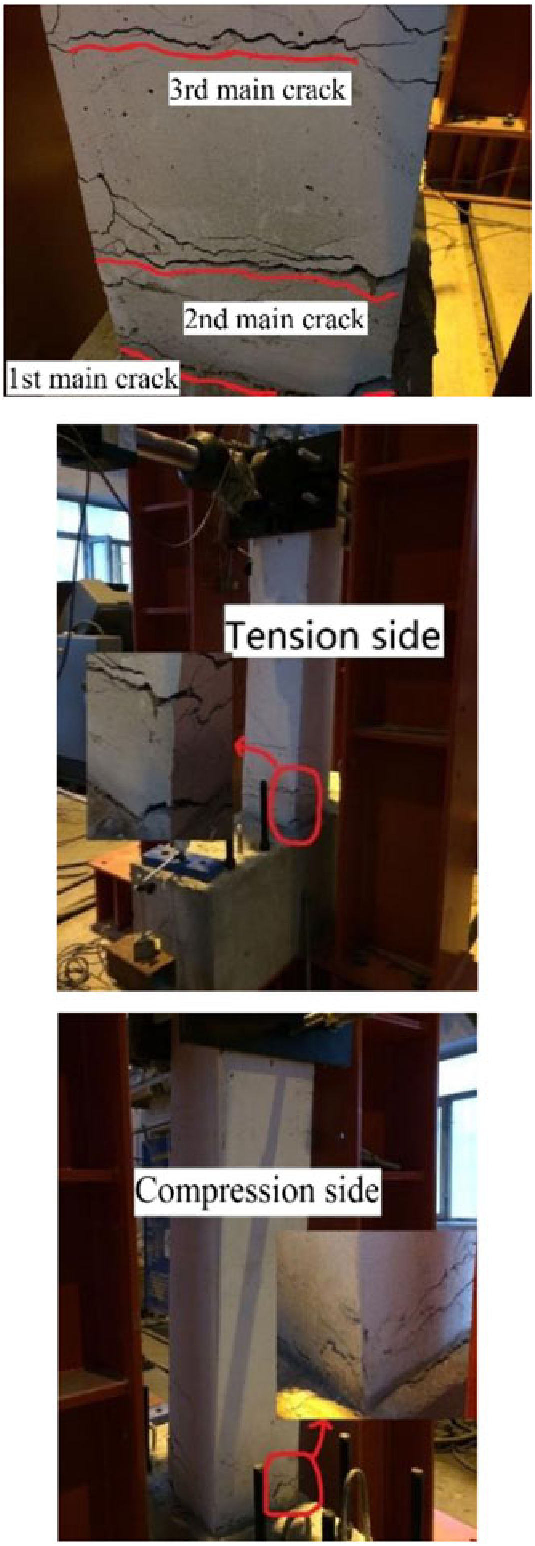

FIGURE 9 Photos of the prototype column after testing

90 MPa. This was caused by the Kent–Scott–Park model, which ignores tensile strength of concrete. In fact, tensile strength plays a significant role in the restoring force of a flexural member when the loading is very limited; if it is ignored, the UKF method will force the compression strength to significantly increase to compensate for the loss of tensile strength.

TABLE 3 Initial and reference values of concrete constitutive law parameters. A hyphen indicates that it is unnecessary (2nd line) or unable (3rd line) to be determined

Parameter	f_{cu} (MPa)	ε_{0u}	f_{ru}	ε_{mu}	K_{sr1}	K_{sr2}	K_{sr3}	f_{yh} (MPa)
Initial value	43	0.002	36.6	0.0038	13.5	40.5	457.8	–
Material (reference) value	43	–	–	–	13.5	–	–	579.9

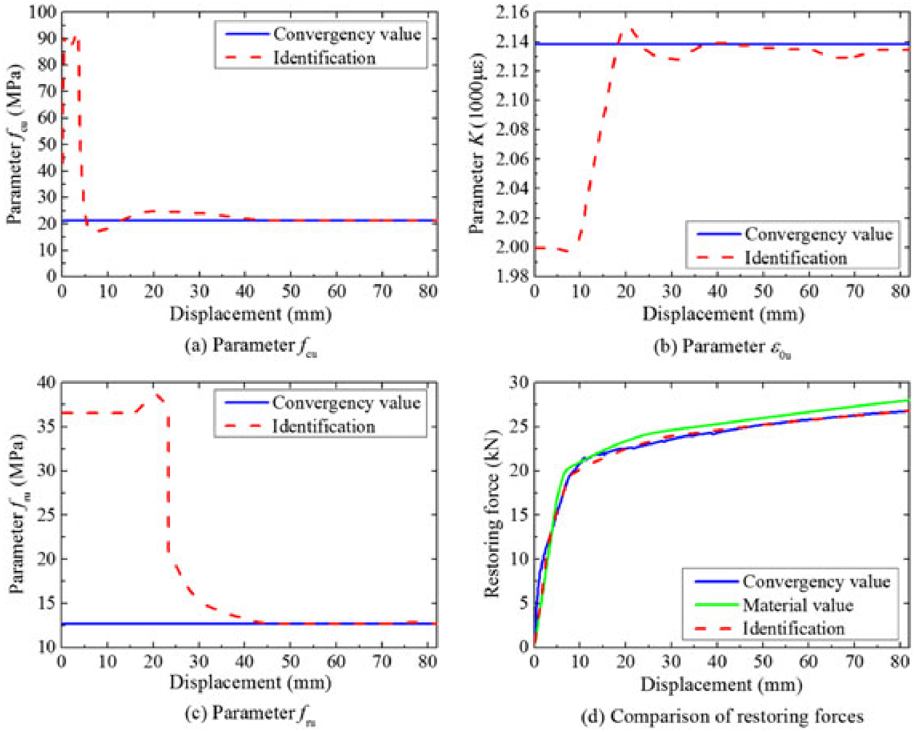

FIGURE 10 Identification results compared with testing measurements

4 | HS WITH ONLINE MODEL UPDATING

In order to validate the effectiveness of the proposed model-updating technique, a HS with and without online model updating was carried out on a one-bay one-story RC frame. Several details of HS and relevant are provided herein.

4.1 | HS framework

The HyTest[33] has been employed hereinafter as a software platform for HS. In greater detail, it performs several functions: (a) control the whole process; (b) solve the system of equations of motion; (c) communicate with the MTS control system linked to the PS, with OpenSEES for NSs and, finally, to Matlab for parameter identification. Figure 11 illustrates the framework of HyTest for HS. There are eight steps involved in HS with model updating that reduce to a standard HS without model updating if only Steps 1, 2, 7, and 8 are carried out. In particular, d defines the displacement provided from the solution of the system of dynamic equations by the COORDINATOR; R_M is the measured force from the PS; R_N represents the calculated force of the NS; R_e is the estimated force from the FE model of the PS, when the identification is triggered; Params defines the identified parameters. With regard to communication, the COORDINATOR is the main server whereas the MTS, OpenSEES, and MATLAB are clients. For the identification part, only MATLAB is the server, and OpenSEES represents the client. In greater detail, for each time step, the COORDINATOR ① sends the displacement to the PS and ② receives the feedback restoring force; ③ sends both displacement and force of the PS to MATLAB and ⑥ receives the identified parameters; ⑦ sends both displacement and parameters to NS and ⑧ receives the calculated force; and it solves the system of equations of motion and proceeds to the next step.

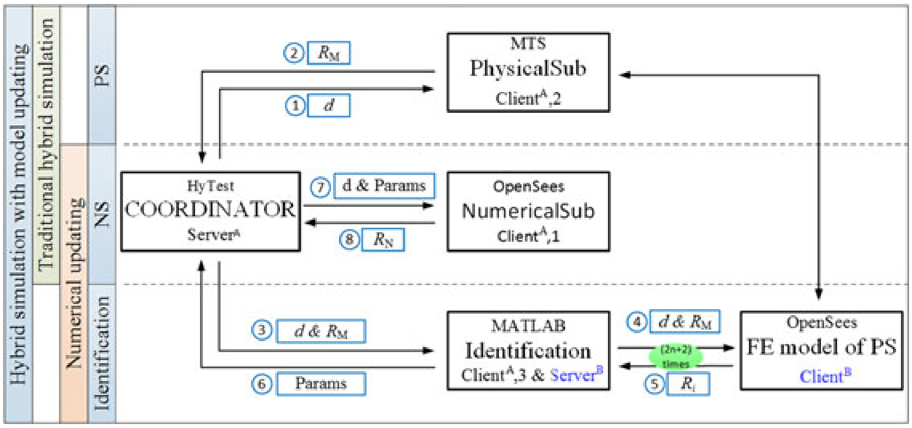

FIGURE 11 Framework of hybrid simulation. FE = finite element; NS = numerical substructure; PS = physical substructure

4.2 | Experimental setup

A one-bay one-story RC frame was selected to be the target structure for HS with model updating as shown in Figure 12. A concentrated mass of 40,000 kg was considered at the top of each end column. The 1/2 scale model of half column on the left was taken as PS whereas the remainder was treated as NSs. Two HS were carried out: (a) one for the case with online model updating and (b) a second one for standard HS w/o model updating. It was assumed that the beam was rigid for axial and bending stiffness; thus, the NS was further simplified with the boundary conditions shown in Figure 13. A force-based beam-column element was built in OpenSEES for the full-scale NS. The cross section of the prototype column was 500 mm × 500 mm whereas the 1/2 scaled PS was the same as that shown in Figure 2. As a result, the test setup was the same as that described in both Figures 7 and 8. The 1940 NS El Centro ground motion was used as seismic input. The damping ratio employed for the frame was 0.05 based on the computed initial stiffness of the frame model; the central difference algorithm was employed for time integration whereas a time step interval of 0.02 s was employed for time-marching scheme.

In the case of HS with updating, the initial values of constitutive law parameters were equal to those for monotonic loading test listed in Table 3. Conversely, in the case of standard HS without model updating, the parameters for the NS were identical to initial values. The initial covariance matrix for UKF was $\text{diag}P_0 = [1.0 \times 10^{-4}\ 1.9 \times 10^{-6}\ 8.9 \times 10^{-4}]$ and $R = 9 \times 10^{-4}$, respectively.

4.3 | Results of HS

The results corresponding to a peak ground acceleration scaled to 0.4 *g* are presented both in Figures 14 and 15. One can observe from these figures, the rapid convergence of the identified parameters to their final values. In particular, Figure 15a shows that the calculated restoring forces with the identified parameters matched quite well with those measured from the PS. In addition, Figure 15b compares the hysteretic loops between the standard HS and the one based on modeling updating (UHS). Their marked difference and the agreement between the UHS-based loops with those of the

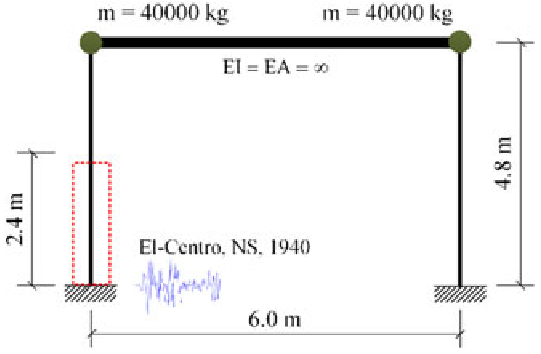

FIGURE 12 Prototype reinforced concrete frame. NS = numerical substructure

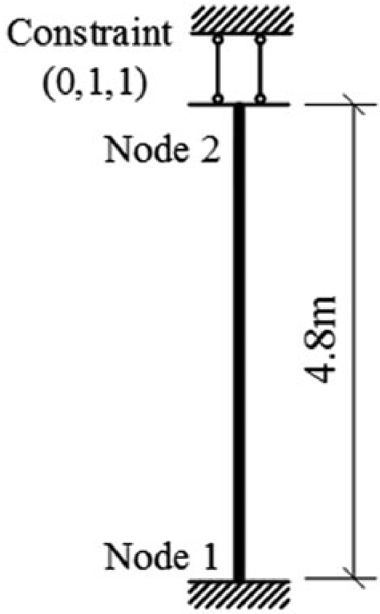

FIGURE 13 Numerically substructured column

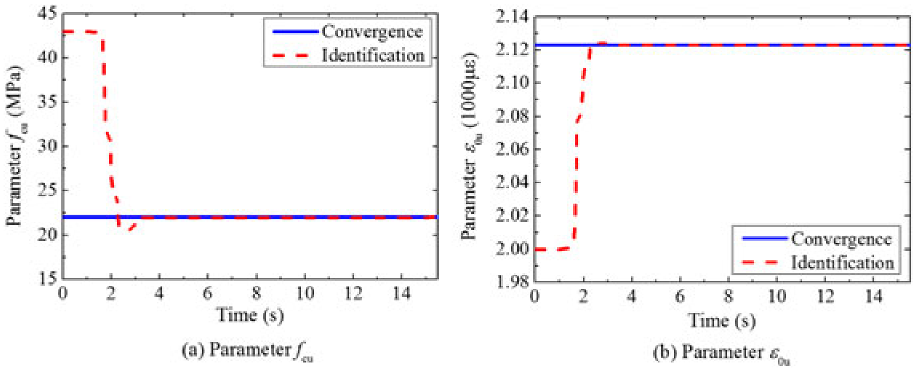

FIGURE 14 Results of parameter identification for a peak ground acceleration = 0.4 *g*

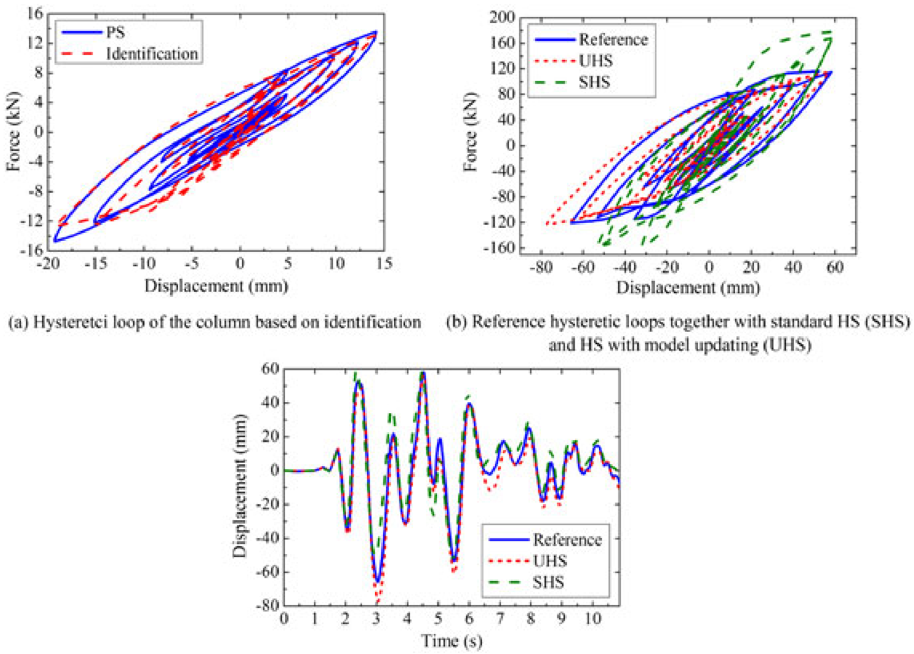

FIGURE 15 Comparisons of frame responses for a peak ground acceleration = 0.4 *g*. PS = physical substructure

reference solution emphasize the advantage of the proposed model updating for RC members. Also, the relevant time histories of Figure 15c highlight the better accuracy achieved by UHS. For clarity, both hysteretic and time histories reference values were computed by OpenSEES using converged constitutive parameters values.

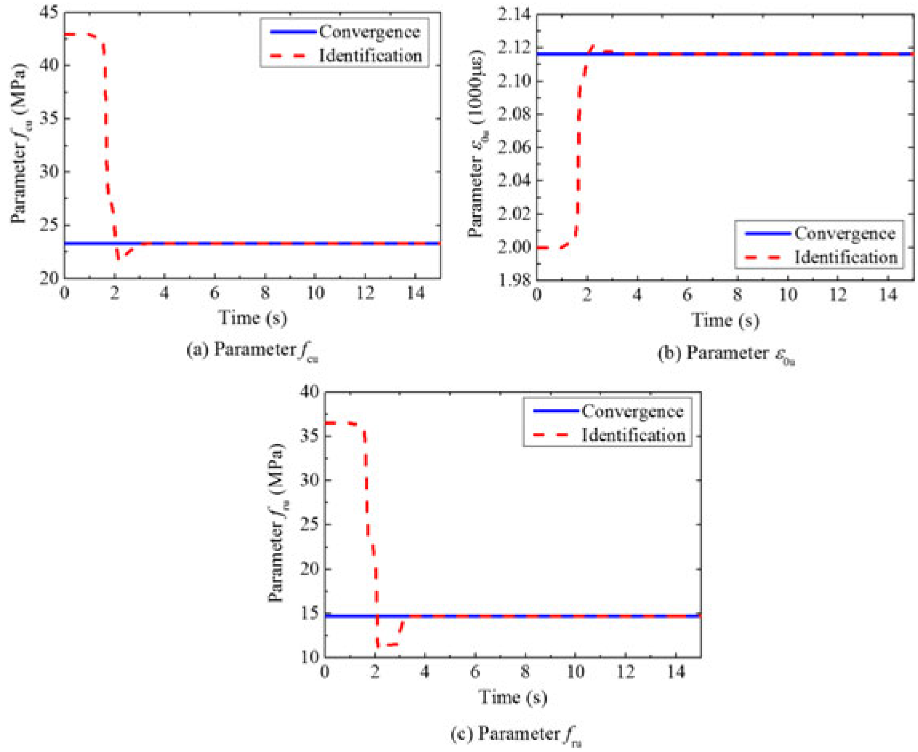

FIGURE 16 Results of parameter identification for a peak ground acceleration = 1 *g*

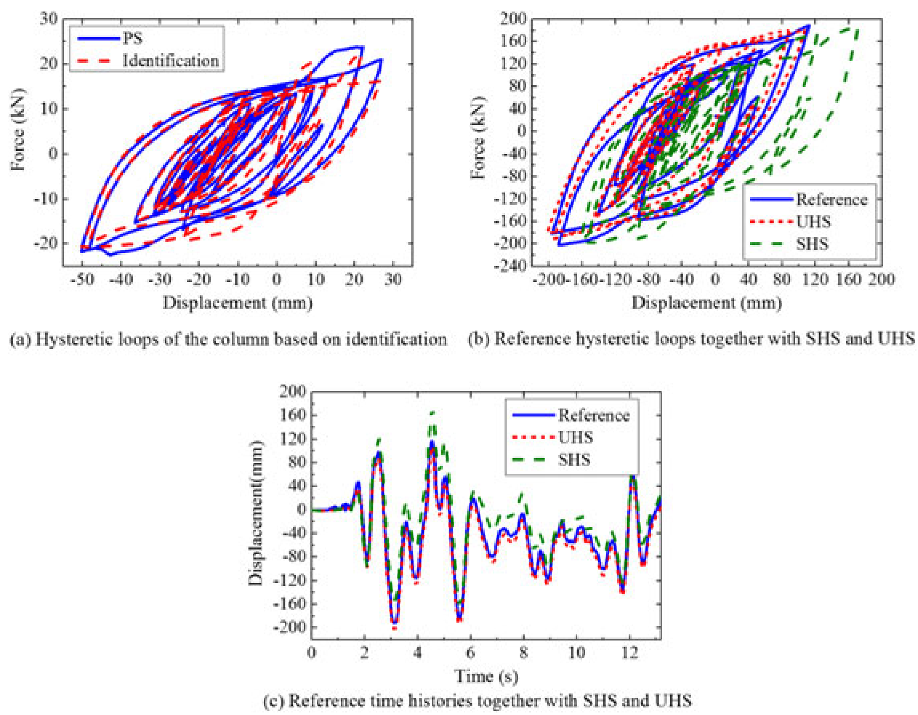

FIGURE 17 Comparisons of frame responses for a peak ground acceleration = 1 *g*. PS = physical substructure

TABLE 4 Convergence value of concrete constitutive parameters. A hyphen indicates that the convergence value of f_{ru} makes no sense in the case of PGA = 0.4 *g*

Case	f_{cu} (MPa)	ε_{0u}	f_{ru} (MPa)
(I) Monotonic test	21.21	0.002138	12.69
(II) PGA = 0.4 *g*	22.01	0.002123	–
(III) PGA = 1 *g*	23.35	0.002116	14.76

TABLE 5 Mean and covariance of identified values

Case	f_{cu} (MPa)	ε_{0u}	f_{ru} (MPa)
Mean	22.19	0.002125	13.73
Standard deviation	1.53	1.59×10^{-5}	1.46

The results corresponding to a peak ground acceleration scaled to 1 *g* are presented both in Figures 16 and 17. Again, the favorable performance of UHS is evident: in the model-updating case (UHS), the results are very close to the reference ones.

For completeness, the final values of identified constitutive law parameters f_{cu}, ε_{0u}, and f_{ru} are provided in Table 4, for the three different test cases discussed above. Their relevant mean and standard deviation are listed in Table 5. It is observed that the identified values of parameters for the three cases are quite close to each other and characterized by small standard deviation. These results justify the reliability of HS based on online model updating. In particular, for the case with 0.4 *g*, the response was not so significant to induce large concrete degradation and, therefore, the parameter f_{ru} remained unchanged as its initial value; thus, it was neither shown in the figures to hand nor listed in Table 4.

5 | CONCLUSIONS

Online model updating represents an effective approach for improving the overall quality of test results that can be implemented in standard HS to improve modeling of critical NSs that cannot be tested in the laboratory, and, hence, the overall quality of test results. In this paper, in order to improve the accuracy of HS, we proposed a model-updating technique applied to concrete constitutive relationships. The UKF was used for parameter estimation of RC constitutive law. It was implemented together with the OpenSEES software and prior to experimental HS, a parametric study of UKF constitutive law parameters was conducted. Successively, the effectiveness of this approach in reducing the overall error compared to a reference response was verified with one analytical example and two tests, that is, a monotonic test on a laterally loaded cantilever column and a HS on a one-bay one-story RC frame. Final values of concrete constitutive relationship parameters generally agreed for each case, thus indicating the reliability of the proposed procedure. In sum, the online updating of constitutive relationships of NSs can effectively extend the applications of conventional HS to systems with several critical members such as multiple-span bridges and complex buildings.

ACKNOWLEDGEMENTS

The authors gratefully acknowledge the financial supports from the National Key Research and Development Program of China (Grant 2016YFC0701106) and the National Natural Science Foundation of China (Grant 51161120360). Moreover, the first author acknowledges the financial support from Seismic Engineering Research Infrastructure for European Synergies (SERIES) Project, funded within the 7th Framework Programme of the European Commission [FP7/2007–2013] under grant agreement 227887, for her research period at the University of Trento, Italy.

REFERENCES

[1] K. Takanashi, K. Udagawa, M. Seki, T. Okada, H. Tanaka, *Bull. Earthquake Resist. Struct. Res. Cent.* **1975**, *8*, 1.

[2] P. Pegon, A. Pinto, *Earthquake Eng. Struct. Dynam.* **2000**, *29*(7), 905.

[3] T. Yang, B. Stojadinovic, J. Moehle, *Earthquake Eng. Struct. Dynam.* **2009**, *38*(1), 95.

[4] A. Calabrese, S. Strano, M. Terzo, *Struct. Control Health Monit.* **2015**, *22*, 535.

[5] A. H. Schellenberg, T. C. Becker, *Struct. Control Health Monit.* **2016**, https://doi.org/10.1002/stc.1915.
[6] T. Horiuchi, M. Inoue, T. Konno, Y. Namita, *Earthquake Eng. Struct. Dynam.* **1999**, *28*(10), 1121.
[7] M. Wallace, J. Sieber, S. Neild, D. Wagg, B. Krauskopf, *Earthquake Eng. Struct. Dynam.* **2005**, *34*(15), 1817.
[8] A. Darby, M. Williams, A. Blakeborough, *J. Eng. Mech.-ASCE.* **2002**, *128*(12), 1276.
[9] C. P. Lamarche, A. Bonelli, O. S. Bursi, *Earthquake Eng. Struct. Dynam.* **2009**, *38*(9), 1071.
[10] B. Wu, G. S. Xu, Q. Y. Wang, M. S. Willianms, *Earthquake Eng. Struct. Dynam.* **2006**, *35*(3), 293.
[11] C. Chen, J. M. Ricles, T. M. Marullo, *Earthquake Eng. Struct. Dynam.* **2009**, *38*(1), 23.
[12] T. Wang, B. Wu, J. Zhang, *Adv. Mater. Res.* **2011**, *250-253*, 2455.
[13] G. Abbiati, O. S. Bursi, P. Caparan, L. D. Sarno, F. J. Molina, F. Paolacci, P. Pegon, *Earthquake Eng. Struct. Dynam.* **2015**, *44*(13), 2221.
[14] Y. Yang, K. Tsai, A. S. Elnashai, T. Hsieh, *Simul. Model. Pract. Th.* **2012**, *28*, 42.
[15] M. J. Hashemi, A. Masroor, G. Mosqueda, *Earthquake Eng. Struct. Dynam.* **2014**, *43*(3), 395.
[16] Y. Nakano, W. J. Yang, *Proceedings of the first international conference on advances in experimental structural engineering* **2005**, *1*, 267.
[17] G. C. Foliente, *J. Struct. Eng.-ASCE.* **1995**, *121*(6), 1013.
[18] Y. Chen, P. Visintin, D. J. Oehlers, U. J. Alengaram, *J. Struct. Eng.-ASCE.* **2013**, *140*(4), 04013088, 1–11.
[19] B. Wu, T. Wang, *Smart Struct. Syst.* **2014**, *14*(6), 1105.
[20] X. Shao, A. Mueller, B. A. Mohammed, *J. Eng. Mech.-ASCE* **2016**, *142*(2), 04015074, 1–19.
[21] B. Wu, Y. Chen, G. Xu, Z. Mei, T. Pan, *Earthquake Eng. Struct. Dynam.* **2016**, *45*, 1251.
[22] R. Kalman, *Transactions ASME. J. Basic Eng.* **1960**, *82D*, 35.
[23] S. Julier, J. Uhlmann, H. Durrant-Whte, *IEEE Trans. Autom. Cont.* **2000**, *45*(3), 477.
[24] E. Wan, V. D. R. Merwe, *IEEE Adapt. Syst. Signal Proc., Commun, and Cont. Symp.* **2000**, 153.
[25] M. Wu, A. W. Smyth, *Struct. Control Health Monit.* **2007**, *14*(7), 971.
[26] S. Mazzoni, F. Mckenna, M. H. Scott, G. L. Fenves, OpenSees command language manual. PEER Center, **2006**.
[27] B. Scott, R. Park, M. Priestley, *Journal Proceedings.* **1982**.
[28] D. C. Kent, R. Park, *J. Struct. Division.* **1971**, *97*(7), 1969.
[29] J. B. Mander, M. J. Priestley, R. Park, *J. Struct. Eng.* **1988**, *114*(8), 1804.
[30] E. Hognestad, *Eng. Exp. Station.* **1951**, *399*.
[31] J. L. Doob, *Stochastic Processes*, Wiley, New York **1953**.
[32] *MATLAB and Statistics Toolbox Release*. The MathWorks, Inc., Natick, Massachusetts, US. **2012**
[33] G. Yang, B. Wu, G. Ou, Z. Wang, S. Dyke, *Adv. Eng. Software*., https://doi.org/10.1016/j.advengsoft.2017.05.007.

How to cite this article: Mei Z, Wu B, Bursi OS, Yang G, Wang Z. Hybrid simulation of structural systems with online updating of concrete constitutive law parameters by unscented Kalman filter. *Struct Control Health Monit*. 2017;e2069. https://doi.org/10.1002/stc.2069

APPENDIX A

A.1 | Relation between f_{cu} and relevant estimated measurements

When the constitutive parameter f_{cu} is the sole parameter to be identified, the relationship between σ and f_{cu} can be simply expressed as

$$\sigma_c = h(\varepsilon_i) \cdot f_{cu} = h_i \cdot f_{cu}. \tag{A.1}$$

The axial force and bending moment in the cross section read,

$$N = \int_A \sigma_c dA + N_s, \tag{A.2}$$

$$M = \int_A z \sigma_c dA + M_s, \tag{A.3}$$

where N_s and M_s are axial force and bending moment provided by steel reinforcing bars (rebars); z is the distance from the neutral axis. Then, the bending moment of the two element nodes can be expressed as

$$M_i = \int_l (a_i N + b_i M) ds \quad i = 1, 2, \tag{A.4}$$

in which l is the height of element; a_i and b_i are the coefficients related to the shape function of element.

The base-shear of the column, that is, the estimated measurement, can be calculated as

$$\hat{y} = (M_1 + M_2)/2 \quad i = 1, 2. \tag{A.5}$$

Substituting (A.1), (A.2), (A.3), and (A.4) into (A.5), one can obtain

$$\hat{y} = H_i \cdot f_{\mathrm{cu}} + R_{\mathrm{s},i},$$

where $R_{\mathrm{s},i}$ is the force exerted by rebars that can be considered to be a constant at each step.

APPENDIX B

B.1 | Monotonic convergence of Kalman filter for a single-parameter identification

According to Section 3, the identified constitutive law parameters are related to the measurement through

$$y_i = H_i \cdot x + C_i, \tag{B.1}$$

where C_i is a constant. The noise is ignored in B.2 to derive the analytical expression of the estimated parameter. Hence, the estimated value of measurement reads,

$$\hat{y}_i = H_i \cdot \hat{x}_i + C_i. \tag{B.2}$$

According to Kalman filter theory,[21] the estimation of x at the i-th step can be obtained by,

$$\hat{x}_i = \hat{x}_{i-1} + K_i (y_i - \hat{y}_i) \tag{B.3}$$

where the Kalman gain is expressed as

$$K_i = \frac{H_i P_{i-1}}{H_i^2 P_{i-1} + R}. \tag{B.4}$$

Substituting B.1 and B.2 into B.3 provides

$$e_i = a e_{i-1} \tag{B.5}$$

in which

$$e_i = \hat{x}_i - x \tag{B.6}$$

and

$$a = \frac{R}{H_i^2 P_{i-1} + R} \tag{B.7}$$

As $0 < a < 1$, e_i as well as $\widehat{x}_i$ will monotonically converge; that entails that the identified f_{cu} value will monotonically approach the reference value. The relevant numerical validation is presented in Figure A1.

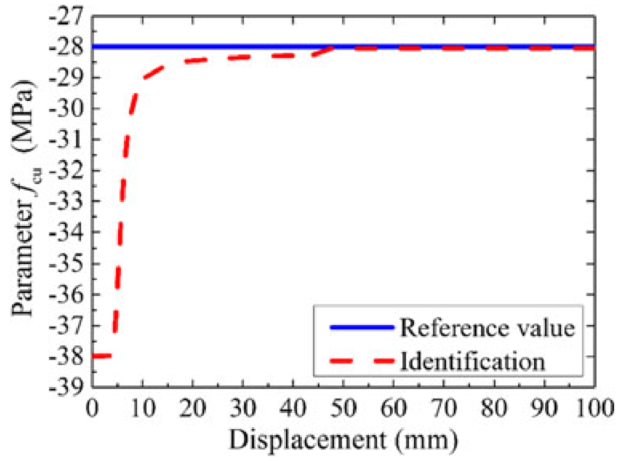

FIGURE A1 Identification of the single parameter f_{cu}

APPENDIX C

C.1 | Overshoot of the identification curve of f_{cu}

On the basis of Appendix B, when only one parameter f_{cu} is identified, no overshoot appears in the identification curve. However, adding the parameter ε_{0u} entails an overshoot to the parameter f_{cu}, and relevant results are shown in Figure A2.

It is evident from Figure 4 that different parameters have different sensitivities to the restoring force; this phenomenon could lead to different convergence rates for each parameter and, hence, could cause a fluctuation in estimation as illustrated in Figure A3.

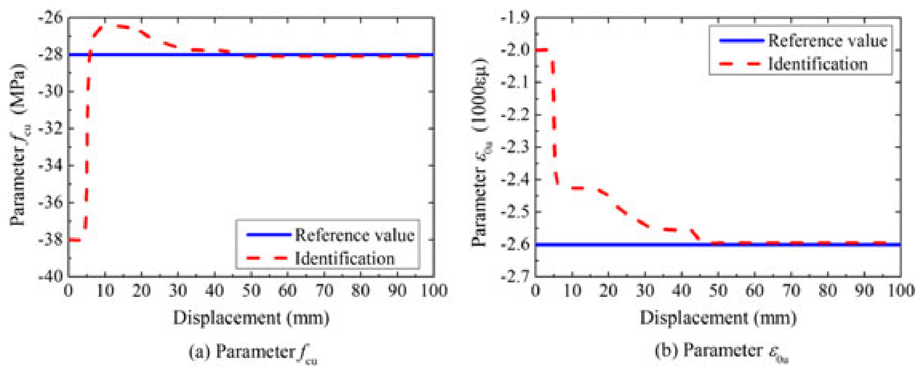

FIGURE A2 Process identification of two concrete constitutive law parameters

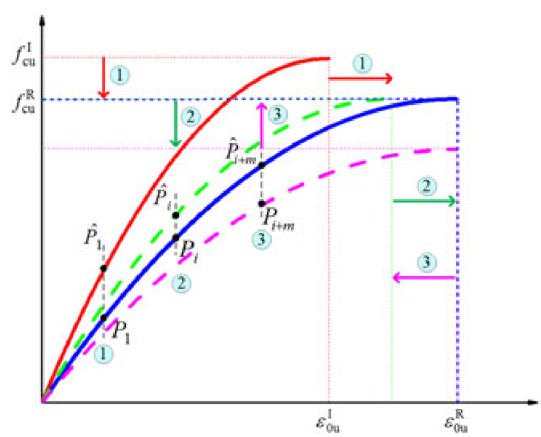

FIGURE A3 Fluctuation of two parameter identification

In particular, the blue curve represents a stress–strain relation determined by the reference values f_{cu}^{Ref} and ε_{0u}^{Ref}, whereas the red curve was determined with the initial values f_{cu}^{I} and ε_{0u}^{I}. In this case, the estimated stress value at the initial step is greater than the measured value, that is, $\widehat{\sigma}_i > \sigma_i$. Then, in subsequent steps, the identified f_{cu} has to decrease and ε_{0u} must increase towards the reference value to allow the estimated stress to approach measurement. As a result, f_{cu} and ε_{0u} may exhibit different convergence rates. Let us assume that the former converges to the reference value faster than the latter, which results in the green curve of Figure A3. As the estimated stress denoted by the green line is still greater than the measured value, f_{cu} should further decrease and ε_{0u} further increase to pull down the estimated stress towards its reference value, which results in the pink curve of Figure A3. Due to error correction property of Kalman-type filter, the estimated stress will converge to the reference value, which will also drive the estimated parameters to converge; as a result, f_{cu} will go back to its previous value. As a result in the identification process, the fluctuation of f_{cu} arises as shown by the vertical arrows numbered ①, ②, and ③.